Log-Skew-Normality of Ocean Turbulence

B. B. Cael*
National Oceanography Centre, Cael SO14 3ZH, Southampton, United Kingdom

Ali Mashayek
Imperial College, Mashayek SW7 2BB, London, United Kingdom

(Received 9 October 2020; revised 12 January 2021; accepted 16 March 2021; published 4 June 2021)

The statistics of intermittent ocean turbulence is the key link between physical understanding of turbulence and its global implications. The log-normal distribution is the standard but imperfect assumed distribution for the turbulent kinetic energy dissipation rate. We argue that as turbulence is often generated by multiple changing sources, a log-skew-normal (LSN) distribution is more appropriate. We show the LSN distribution agrees excellently and robustly with observations. The heavy tail of the LSN distribution has important implications for sampling of turbulence in terrestrial and extraterrestrial analogous systems.

DOI: 10.1103/PhysRevLett.126.224502

Introduction.—Turbulence induced by breaking waves is an abundant feature of many terrestrial and extraterrestrial systems, occurring over a tremendous range of scales. Shear-induced turbulence leads to efficient mixing of important properties such as temperature and carbon in the ocean and atmosphere [1,2]; to the magnetic reconnection by which solar wind plasma enters Earth's magnetosphere [3]; to mixing of magnetized plasma in planetary, solar, or stellar environments [4–9]; and to homogenization of gases in interstellar media, for example, in nova explosions [10]. In all these contexts, turbulence is highly spatiotemporally intermittent. Therefore, sufficient sampling of such turbulence, to the extent necessary for quantification of properties of interest such as turbulent mixing, is difficult and in many cases impossible. Oceanic wave–induced turbulence is among the better sampled and studied of the aforementioned applications because of its critical role in the climate system. In this Letter we draw on a wide range of oceanic turbulence measurements to highlight a seeming universality to shear-induced turbulence statistics that we expect is relevant to other physical media.

Over the past century, there has been significant progress in our understanding of the physics of wave-induced turbulent mixing [11] and of the role of small-scale mixing in large-scale circulation [12]. But there has arguably been a systematic disconnect between the fluid-mechanical studies of the former and the physical-oceanographic studies of the latter because of the high spatiotemporal intermittency of ocean turbulence. While effective on global and climatic timescales, mixing occurs on scales of subcentimeters to tens of meters and is highly intermittent due to the variable nature of the forcing, namely the air-sea interaction and the interactions of tides and geostrophic motions with topography (see Fig. 1 for associated global patterns). Thus, connecting the microphysics of mixing to the ocean circulation is challenging because of the substantial scale separation, in a fashion similar to the relevance of cloud microphysics to the climate system [13]. Apart from deep convection zones at high latitudes, the ocean interior can sustain an internal wave field, being mostly stably stratified. However, occasional turbulence bursts due to propagating waves breaking generate local turbulence patches that mix dense deeper waters with lighter waters above. These patches are more frequent closer to ocean boundaries where winds and topographic interactions generate a strong internal wave field. Such waves contribute to local breaking due to many interactions between the waves, eddies, and currents, but also propagate into the interior, where they can lead to more intermittent breaking.

Sampling of wave breaking is costly and poses many technical challenges [17,18], especially in the deep and abyssal ocean. Nonetheless, the data from 14 major field programs that sampled ocean turbulence over shallow and deep regions using microstructure profilers [Fig. 1(a), Table I] have been compiled at [19]; data description and relevant references may be found in [20]. Together, they contain ca. 186 000 turbulent samples (with 10 m vertical resolution) spanning the globe, ocean depths, and various turbulence regimes. While no such dataset can be a truly comprehensive representation of ocean turbulence, this is a sufficiently large and diverse sample set to provide

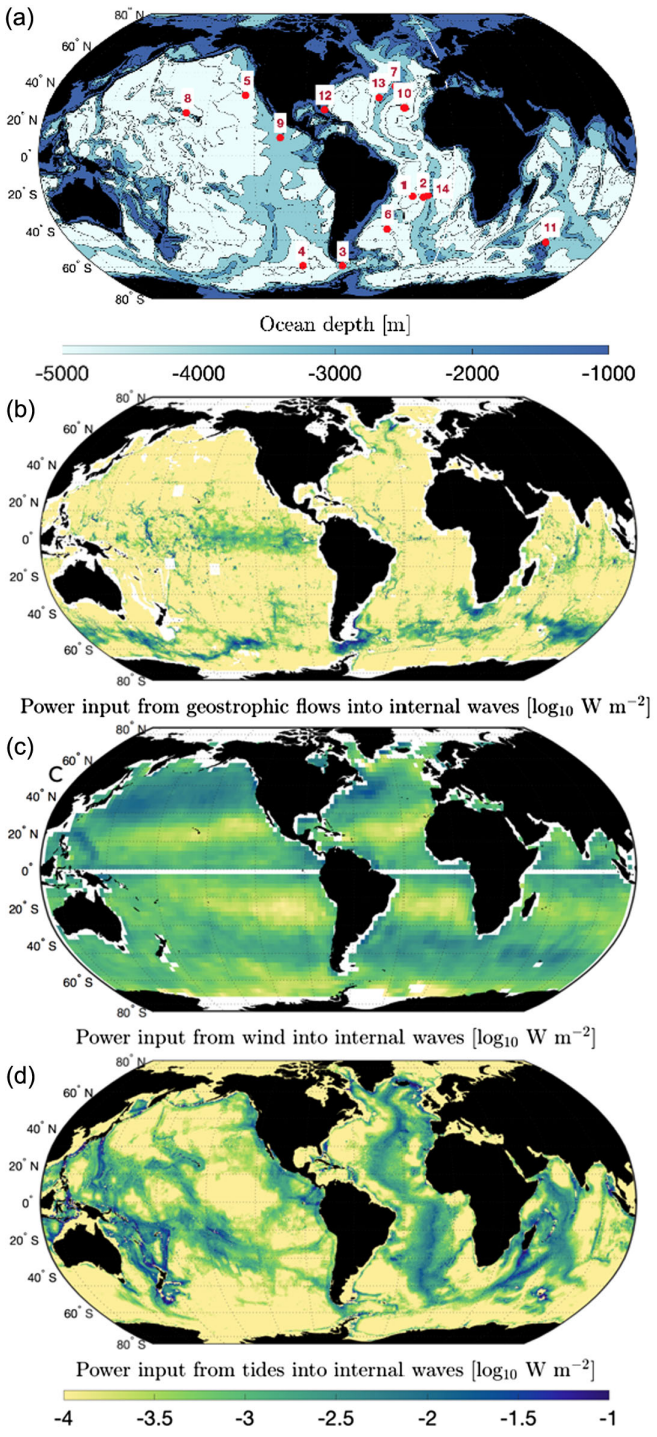

FIG. 1. (a) Ocean bathymetry overlain by location of the field programs listed in Table I. (b) Primary sources of generation of internal waves through interaction of geostrophic motions with topography [14]. (c) Surface winds [15]. (d) Tide-topography interaction [16].

the statistics required to make a connection between the physics of small scale turbulence and the role of mixing in a bulk regional or global sense. The dataset contains values for the rate of dissipation of kinetic energy ε inferred from profiled measurements of microscale shear. ε is used as a proxy of ocean turbulent mixing $\mathcal{M}$ and is related to it through $\mathcal{M} \approx \kappa N^2 \approx \Gamma\varepsilon$, where $N^2 = -(g/\rho_0)\partial_z\rho$ represents the density stratification, g is the gravitational constant, and ρ_0 is a reference density [21]. The turbulent diffusivity κ is a necessary parameter in climate models to represent unresolved turbulent mixing. Γ is a coefficient at the heart of connecting ε and $\mathcal{M}$ and is highly variable [22,23] with appreciable consequences [24–26]. While the assumptions underlying the derivation of this mixing equation are limiting [21,22,27], operationally this equation with $\Gamma = 0.2$ is used in observational inferences and computational representations of mixing.

To better understand the limitations of the underlying assumptions in this equation, better parametrize Γ, connect localized inferences of mixing to coarse resolution grids of ocean models, and ultimately more accurately quantify the role of ocean mixing in the climate system, the intermittency of ocean turbulence and its statistics must be much better understood. In this Letter we employ the database in Table I and show that the discrepancy between the observed ε distribution(s) and the conventional paradigm of a log-normal ε distribution is resolved by a generalization that considers turbulence to be generated by multiple or changing sources. While the log-normal paradigm has been challenged in the past (e.g., [28]), we provide a simple explanation for a generalization that fits not only the

TABLE I. Kuiper's statistic (V) for log-normal (LN) and log-skew-normal (LSN) fits to the total turbulent dissipation rate (ε) dataset, the dataset normalized by buoyancy frequency (N^2), the total dataset above and below 2000 m, and data from each individual cruise, as well as their log-mean (μ), log-standard deviation (σ), and log-skewness (θ) of the $\log_{10}$-transformed data. n.b. there are fewer ε/N^2 values because some ε values come from samples where $N^2 \approx 0$.

Data	$n/10^3$	V_{LN}	V_{LSN}	μ	σ	θ
All	186	0.123	0.020	−9.75	0.73	0.64
$z < 2$ km	116	0.129	0.021	−9.58	0.73	0.62
$z > 2$ km	70	0.145	0.034	−10.04	0.63	0.63
1. BBTRE96	32	0.158	0.025	−9.88	0.57	0.88
2. BBTRE97	39	0.087	0.026	−9.70	0.69	0.71
3. DIMES	3	0.209	0.035	−9.45	0.58	0.93
4. DIMES-Pac.	16	0.118	0.016	−9.98	0.26	0.90
5. Fieberling	11	0.079	0.069	−9.15	0.82	0.90
6. GEOTRACES	7	0.130	0.039	−10.10	0.69	0.88
7. GRAVILUCK	2	0.092	0.054	−9.02	0.61	0.80
8. HOME	4	0.204	0.019	−7.90	0.57	0.90
9. LADDER	9	0.210	0.031	−9.94	0.31	0.88
10. NATRE	27	0.074	0.021	−9.83	0.55	0.62
11. SOFINE	11	0.174	0.042	−9.22	0.59	0.89
12. TOTO	4	0.184	0.021	−9.54	0.57	0.58
13. RIDGEMIX	7	0.202	0.044	−9.97	0.65	0.91
14. DOMORE	13	0.156	0.015	−10.47	0.62	0.93
All, ϵ/N^2	132	0.085	0.012	−4.24	0.75	0.58

totality of this extensive global dataset but also individual datasets with different primary turbulence generation processes.

Log-skew-normality.—Fluctuations in the turbulent dissipation rate ε are typically parametrized as log-normal; originally Gurvich and Yaglom [29] argued for this based on multistage subdivisions of an initial flux for 3D homogeneous isotropic turbulence (following Kolmogorov's theory), but an analogous argument has also been proposed for larger-scale quasigeostrophic turbulence [30]. It has long been recognized that ε varies over orders of magnitude and has a unimodally distributed logarithm, but also only approximately, qualitatively consistent with a log-normal description [31]. The lack of quantitative agreement has led to an under-reporting of the statistics of turbulence measurements, and has substantial consequences for the total turbulent dissipation because of the heavy-tailed nature of the distribution [32]. These quantitative differences have been attributed to measurement artifacts [33] or to self-similarity–based arguments for multifractality (e.g., [34]) but the log-normal distribution remains popular and argued for in the ocean turbulence literature (e.g., [35]). The key assumption to derive a log-normal ε distribution is that individual instances are derived from a single statistically steady source [36]; consistent with this, the log-normal tends to match ε data from locations where, e.g., single wave breakings in otherwise nearly quiescent environments can lead to isolated shear instabilities that dissipate separately [37,38]. However, total turbulent dissipation is typically the result of a combination of multiple turbulent processes, for which the log-normal distribution is not an appropriate model. As stated by Caldwell and Moum [39], "a log-normal distribution should not be expected when turbulence production is due to more than one source, or to a changing source"—though what distribution to expect instead is unclear. This suggests that generally for energetic ocean turbulent zones we should expect ε to be the sum of log-normal variables, as several interactive turbulence processes are at play.

Sums of log-normals occur frequently in communications problems when one is interested in total interference; in this case it has been shown that sums of log-normal random variables, even correlated ones, are excellently approximated by a log-skew-normal distribution [40–43]: $f(\varepsilon;\xi,\omega,\alpha) = (2/\omega\varepsilon)\phi(\log\varepsilon - \xi/\omega)\varphi[\alpha(\log\varepsilon - \xi/\omega)]$, where f is a probability density function and ϕ and φ, respectively, are the probability and cumulative density functions of a standard Gaussian random variable. (Here and throughout this Letter we consistently refer to $\log_{10}$ rather than $\log_e$ when we discuss log-transformation, log-moments, etc.) This is a generalization of the log-normal distribution where the relationship between the log-skewness (θ) of the distribution and the additional shape parameter α is one to one. The parameters (ξ, ω, α) are related to the log-mean, log-standard deviation, and log-skewness (μ, σ, θ) of a log-skew-normal random variable according to the equations $\mu = \xi + \sqrt{2/\pi}\omega\delta$, where $\delta = \alpha/\sqrt{1+\alpha^2}$; $\sigma = \omega\sqrt{1-(2/\pi)\delta^2}$; and $\theta = (4-\pi)(\sqrt{2/\pi}\delta)^3/\{2[1-(2/\pi)\delta^2]^{3/2}\}$. As the implications of these log-moments' magnitudes (μ, σ, θ) are more intuitive and the parameters (ξ, ω, α) can be easily found by backtransforming these equations, we focus on the log-moments. θ (and hence α) is positively related to the number of log-normals being summed over and the variance in the log-variances of these distributions—that is, summing over more log-normal random variables or log-normal random variables with more differing log-variances will produce more positively skewed distributions—and is also influenced by the correlation structure of the random variables being summed over [41,43]. In Ref. [44] we have provided an example script that builds intuition as to how log-skew-normality emerges from summing log-normals, and how the log-skew-normal's log-moments and parameters depend on the parameters and the number of the underlying log-normal distributions.

Given that total ε is determined by a combination of turbulence-generating processes for which log-normal arguments may be individually valid, and that ε data tend to appear qualitatively similar to a log-normal but often are skewed after log transformation, one might expect these to be excellently described as log-skew-normal. By analogy with the log-skew-normal's use in communications, an individual ε value will be the sum of multiple log-normally varying power inputs. We show this is indeed the case, and discuss the implications for the importance of extreme values and for connecting bulk turbulence budgets to individual processes.

Results.—We fit a log-skew-normal distribution to the cruise data described above, by finding the parameter combinations that minimize Kuiper's statistic [45]: $V_h = \max[F(\varepsilon) - F_h(\varepsilon)] + \max[F_h(\varepsilon) - F(\varepsilon)]$, where F is the cumulative distribution function (CDF) of the ε data and F_h is a hypothesized distribution such as a log-skew-normal; hence smaller Vs indicate better fits. We do the same for a log-normal distribution. Kuiper's statistic V is preferred to the more standard Kolmogorov-Smirnov statistic, as it weights all data equally, rather than weighting toward the median [45,46]. We fit the full dataset, then split it into "upper"and "lower" halves of the ocean (split at 2 km, marking the approximate mean depth of ocean ridges: separating at 200 m, 500 m, and 1 km yielded similar results) which are separately influenced by surface and bottom-generated turbulent processes. We also fit to individual cruises' data. Finally, we also fit the ratio of ε/N^2 for the global dataset, since it has been shown that global distribution of ε scales very well in depth with density stratification [47].

We find the log-skew-normal distribution agrees very well with the full dataset, both for ε and even more so for ε/N^2 (Fig. 2). For multiple reasons including the very large

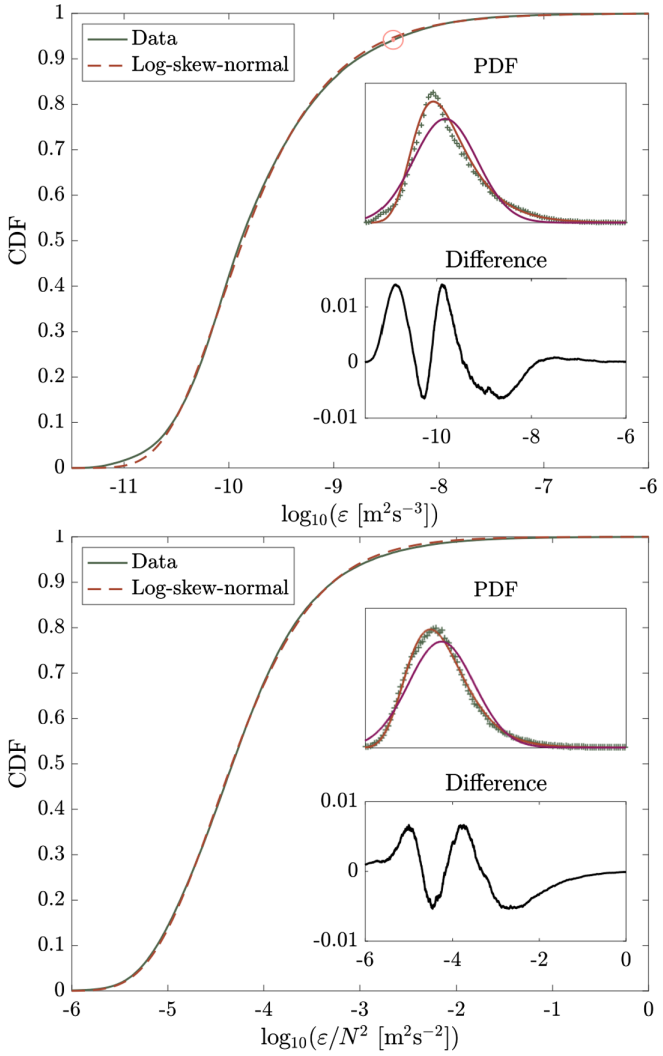

FIG. 2. Cumulative distribution functions (CDFs) of turbulent dissipation measurements (top: ε [$\mathrm{m^2\,s^{-3}}$]) and normalized by buoyancy frequency (bottom: ε/N^2 [$\mathrm{m^2\,s^{-2}}$]) in the dataset described in the text and log-skew-normal (LSN) fit. Insets show corresponding probability density functions and differences between data and LSN CDFs. The purple lines in the top insets are the best fit log-normal distributions for comparison. The pink point in the top figure is 94th percentile; ε values larger than this account for 94% of the total turbulent dissipation in the dataset.

sample size, it is difficult to translate these goodness-of-fit values into meaningful probabilities (i.e., p values, [48]), it is visually evident that the fits are excellent in both cases. Furthermore, the log-skew-normal also vastly outperforms the log-normal, as would be expected from these data having log-skewnesses of $\theta \sim 1$.

Table I summarizes the results from the totality as well as different subsets of the dataset. We find the log-skew-normal to be an improvement over the log-normal in every case (necessarily), and a substantial improvement in almost all cases, with a median difference V_{LN} of 0.108 as compared to a median V_{LSN} of 0.025. Unsurprisingly, more skewed samples have larger differences in goodness-of-fit; log-skewness θ is correlated with V_{LN} and with $V_{\mathrm{LN}} - V_{\mathrm{LSN}}$ ($p < 0.01$, Spearman's rank correlation). Sample size is also significantly anticorrelated with V_{LSN} ($p = 0.049$, Spearman's rank correlation) indicating poorer fits may be due in part to limited sample sizes. As seen in Fig. 2, the better log-skew-normal fit to ε/N^2 than to ε is due to the former having a broader peak, which is unsurprising given that it is the quotient of random variables. Log-skewness and log-kurtosis of the ε distributions are also very tightly related ($\rho > 0.99$, Pearson correlation), further indicating that the log-skew-normal is a satisfactory description of these data, as they are fully characterized by these three log-moments.

The devil is in the tail.—The positive log-skewness of the ε distributions also has key consequences for the importance of extreme ε values to total dissipation. This can be concisely summarized in terms of the "80/20" rule: for the log-skew-normal distribution with parameters chosen to match the total ε dataset, 94% of total turbulent dissipation is contained in the largest 6% of the measurements (Table I; Fig. 3). (For the measurements themselves, 93% of the total turbulent dissipation is contained in the largest 7% of the measurements; small discrepancies in exact values are sensitive to the magnitudes of the few very largest measurements.) By contrast, the best fit log-normal distribution has a very different tail importance, with 80% of the total turbulent dissipation contained in the largest 20% of the measurements. Thus a log-skew-normal of these data suggests much more strongly that extreme ε values are responsible for nearly all of the total turbulent dissipation than a log-normal conceptualization would suggest. This also indicates both that the extremely high ε values occasionally observed are likely real, and not erroneous or anomalous, and also that with a finite number of observations even if the exact shape of the distribution is captured it will be difficult to determine total dissipation because this will be very sensitive to the exact values this distribution's (uncertain) parameters, especially the parameter controlling the heavy tail, i.e., θ (or α).

Climate models are often fed with total turbulent dissipation over a large volume (call this $\mathcal{E}$), such as a model

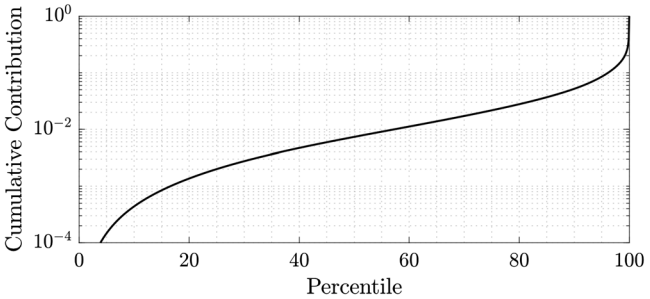

FIG. 3. Cumulative contribution to total ε versus percentile for the total dataset.

grid cell, from the power inputs of various turbulence-generating processes [Figs. 1(b)–1(d)], then rely on bulk parametrizations of Γ to convert $\mathcal{E}$ to, e.g., the mixing of interest [26]. In contrast to this coarse conversion, knowledge of ε or ε/N^2's probability distribution in a given volume is a critical piece in the rigorous calculation of the ocean mixing occurring within that volume. From this distribution and total $\mathcal{E}$ for a volume, one can infer the distribution of turbulent patches within a given volume and infer their mixing characteristics (such as its efficiency and the effective turbulent diffusivity) through our mechanistic and fluid mechanical understanding of mixing. In Ref. [44] we have provided an example script that converts the total dissipation in the volume of an energetic ocean zone [corresponding to DIMES (experiment 3 in Table I)] into a log-skew-normal volume distribution of ε/N^2 values, which can then be directly input into a mixing scheme.

Altogether, the log-skew-normal distribution is a substantially improved description of rate of dissipation of kinetic energy. Log-skew-normality arises because measured dissipation rates are generated by multiple and/or time-varying sources. We note that while skewed distributions of ε have been previously reported for oceanic applications (e.g., see [28] and references therein), we offer a new distribution, and more importantly, one that we can understand on physical grounds. Furthermore, we use an extensive collection of oceanic data (for the purposes of our topic) to show that our reasoning holds for turbulence generated by many different processes from the winds at the ocean surface to by tides and other processes in the abyssal ocean and in between.

Since log-skew-normal distributions have significantly heavier tails in the strong turbulent regime, it implies the need for higher sampling rates to capture the extreme values that make a disproportionately larger contribution to turbulent properties such as mixing. In the oceanic context, we are most often significantly undersampling turbulence. The sampling issue is even graver for extraterrestrial applications. But the seeming universality of distribution of ε provides a practical way toward interpretation of sparse data. One can, for instance, estimate log-skew-normal distribution parameters (with uncertainties) from a sample set, and use that distribution's mean and its uncertainty in place of the sample mean and its uncertainty, thereby more effectively using the total dataset to constrain the mean, rather than essentially just the few largest values.

The rate of dissipation of turbulent kinetic energy and velocity shear are universal properties of all turbulent flows. Where wave-induced turbulence plays an important role, the seeming universality of distribution of ε, which solely relies on existence of various wave-generating processes and interaction among them, likely transcends the oceanic applications and can potentially help interpret hardly sought yet sparse observations in planetary physics and astronomy. This expectation is further reinforced by the similarity of the mathematically analogous magneto-hydrodynamics physics in planetary, stellar, and astrophysical contexts and the density stratified turbulence in the ocean: in the former, the magnetic field provides a stratification that induces, suppresses, and in return gets mixed by wave-induced turbulence, while in the ocean and atmosphere, the gravitational field of Earth facilitates similar dynamics.

All code will be made available [44].

It is a pleasure to thank Laura Cimoli for help with reproducing maps from Cimoli *et al.* [26] for Fig. 1 and Matthew Alford and two anonymous reviewers for their insightful suggestions on previous drafts of this Letter. B. B. C. acknowledges support from the National Environmental Research Council (NE/R015953/1) and the Horizon 2020 Framework Programme (820989, project COMFORT, our common future ocean in the Earth system quantifying coupled cycles of carbon, oxygen, and nutrients for determining and achieving safe operating spaces with respect to tipping points). A. M. acknowledges support from National Environmental Research Council (NE/P018319/1). The work reflects only the authors' view; the European Commission and their executive agency are not responsible for any use that may be made of the information the work contains.

B. B. C. and A. M. contributed equally to this work.

*cael@noc.ac.uk

[1] L. D. Talley *et al.*, Changes in ocean heat, carbon content, and ventilation: a review of the first decade of GO-SHIP global repeat hydrography, Annu. Rev. Mar. Sci. **8**, 185 (2016).

[2] D. C. Fritts, C. Bizon, J. A. Werne, and C. K. Meyer, Layering accompanying turbulence generation due to shear instability and gravity-wave breaking, J. Geophys. Res. Atmos. (1984–2012) **108**, 8452 (2003).

[3] S. Kavosi and J. Raeder, Ubiquity of Kelvin–Helmholtz waves at Earth's magnetopause, Nat. Commun. **6**, 7019 (2015).

[4] H. Hasegawa, M. Fujimoto, T.-D. Phan, H. Reme, A. Balogh, M. Dunlop, C. Hashimoto, and R. TanDokoro, Transport of solar wind into Earth's magnetosphere through rolled-up Kelvin–Helmholtz vortices, Nature (London) **430**, 755 (2004).

[5] R. Prangé, L. Pallier, K. C. Hansen, R. Howard, A. Vourlidas, R. Courtin, and C. Parkinson, An interplanetary shock traced by planetary auroral storms from the Sun to Saturn, Nature (London) **432**, 78 (2004).

[6] H. Isobe, T. Miyagoshi, K. Shibata, and T. Yokoyama, Filamentary structure on the Sun from the magnetic Rayleigh–Taylor instability, Nature (London) **434**, 478 (2005).

[7] J. Paral and R. Rankin, Dawn–dusk asymmetry in the Kelvin–Helmholtz instability at Mercury, Nat. Commun. **4**, 1645 (2013).

[8] L. Sorriso-Valvo, F. Catapano, A. Retinò, O. Le Contel, D. Perrone, O. W. Roberts, J. T. Coburn, V. Panebianco, F. Valentini, S. Perri *et al.*, Turbulence-Driven Ion Beams in the Magnetospheric Kelvin-Helmholtz Instability, Phys. Rev. Lett. **122**, 035102 (2019).

[9] A. Beresnyak, Mhd turbulence, Living Rev. Comput. Astrophys. **5**, 2 (2019).

[10] J. Casanova, J. José, E. García-Berro, S. N. Shore, and A. C. Calder, Kelvin–Helmholtz instabilities as the source of inhomogeneous mixing in nova explosions, Nature (London) **478**, 490 (2011).

[11] C. P. Caulfield, Layering, instabilities, and mixing in turbulent stratified flows, Annu. Rev. Fluid Mech. **7**, 113 (2020).

[12] C. Wunsch and R. Ferrari, Vertical mixing, energy, and the general circulation of the oceans, Annu. Rev. Fluid Mech. **36**, 281 (2004).

[13] M. Baker, Cloud microphysics and climate, Science **276**, 1072 (1997).

[14] M. Nikurashin and R. Ferrari, Overturning circulation driven by breaking internal waves, J. Phys. Oceanogr. **40**, 3133 (2013).

[15] M. H. Alford, J. A. MacKinnon, H. L. Simmons, and J. D. Nash, Near-inertial internal gravity waves in the ocean, Annu. Rev. Mar. Sci. **8**, 95 (2016).

[16] C. Vic, A. C. Naveira Garabato, J. A. Green, A. F. Waterhouse, Z. Zhao, A. Melet, C. de Lavergne, M. C. Buijsman, and G. R. Stephenson, Deep-ocean mixing driven by small-scale internal tides, Nat. Commun. **10**, 2099 (2019).

[17] E. L. Shroyer, J. D. Nash, A. F. Waterhouse, and J. N. Moum, in *Measuring Ocean Turbulence* (Springer, Cham, 2018), pp. 99–122.

[18] S. A. Thorpe, *The Turbulent Ocean* (Cambridge University Press, Cambridge, 2005).

[19] https://microstructure.ucsd.edu.

[20] A. F. Waterhouse, J. A. MacKinnon, J. D. Nash, M. H. Alford, E. Kunze, H. L. Simmons, K. L. Polzin, L. C. St. Laurent, O. M. Sun, R. Pinkel, and others, Global patterns of diapycnal mixing from measurements of the turbulent dissipation rate, J. Phys. Oceanogr. **44**, 1854 (2014).

[21] T. R. Osborn, Estimates of the local rate of vertical diffusion from dissipation measurements, J. Phys. Oceanogr. **10**, 83 (1980).

[22] A. Mashayek and W. R. Peltier, Shear-induced mixing in geophysical flows: does the route to turbulence matter to its efficiency? J. Fluid Mech. **725**, 216 (2013).

[23] M. Gregg, E. D'Asaro, J. Riley, and E. Kunze, Mixing efficiency in the ocean, Annu. Rev. Mar. Sci. **10**, 443 (2018).

[24] C. de Lavergne, G. Madec, J. Le Sommer, A. J. G. Nurser, and A. C. Naveira Garabato, The impact of a variable mixing efficiency on the abyssal overturning, J. Phys. Oceanogr. **46**, 663 (2015).

[25] A. Mashayek, H. Salehipour, D. Bouffard, C. P. Caulfield, R. Ferrari, M. Nikurashin, W. R. Peltier, and W. D. Smyth, Efficiency of turbulent mixing in the abyssal ocean circulation, Geophys. Res. Lett. **44**, 6296 (2017).

[26] L. Cimoli, C. P. Caulfield, H. L. Johnson, D. P. Marshall, A. Mashayek, A. C. Naveira Garabato, and C. Vic, Sensitivity of deep ocean mixing to local internal tide breaking and mixing efficiency, Geophys. Res. Lett. **46**, 14622 (2019).

[27] A. Mashayek, C. P. Caulfield, and W. R. Peltier, Time-dependent, non-monotonic mixing in stratified turbulent shear flows: implications for oceanographic estimates of buoyancy flux, J. Fluid Mech. **736**, 570 (2013).

[28] I. Lozovatsky, H. Fernando, J. Planella-Morato, Z. Liu, J.-H. Lee, and S. Jinadasa, Probability distribution of turbulent kinetic energy dissipation rate in ocean: observations and approximations, J. Geophys. Res. **122**, 8293 (2017).

[29] A. S. Gurvich and A. M. Yaglom, Breakdown of eddies and probability distributions for small-scale turbulence, Phys. Fluids **10**, S59 (1967).

[30] B. Pearson and B. Fox-Kemper, Log-Normal Turbulence Dissipation in Global Ocean Models, Phys. Rev. Lett. **120**, 094501 (2018).

[31] R. W. Stewart, Turbulence and waves in a stratified atmosphere, Radio Sci. **4**, 1269 (1969).

[32] J. N. Moum and T. P. Rippeth, Do observations adequately resolve the natural variability of oceanic turbulence? J. Mar. Syst. **77**, 409 (2009).

[33] M. A. Baker and C. H. Gibson, Sampling of turbulence in the stratified ocean, J. Phys. Oceanogr. **17**, 1817 (1987).

[34] K. R. Sreenivasan and C. Meneveau, The multifractal nature of turbulent energy dissipation, J. Fluid Mech. **224**, 429 (1991).

[35] K. Huguenard, K. Bears, and B. Lieberthal, Intermittency in estuarine turbulence: a framework toward limiting bias in microstructure measurements, J. Atmos. Ocean. Technol. **36**, 1917 (2019).

[36] H. Yamazaki and R. Lueck, Why oceanic dissipation rates are not lognormal, J. Phys. Oceanogr. **20**, 1907 (1990).

[37] H. van Haren and L. Gostiaux, A deep-ocean (Kelvin-Helmholtz) billow train, Geophys. Res. Lett. **37**, L03605 (2010).

[38] M. C. Gregg, Scaling turbulent dissipation in the thermocline, J. Geophys. Res. **94**, 9686 (1989).

[39] D. R. Caldwell and J. N. Moum, Turbulence and mixing in the ocean, Rev. Geophys. **33**, 1385 (1995).

[40] M. B. Hcine and R. Bouallegue, Fitting the log skew normal to the sum of independent lognormals distribution, arXiv:1501.02344.

[41] M. B. Hcine and R. Bouallegue, Highly accurate log skew normal approximation to the sum of correlated lognormals, arXiv:1501.02347.

[42] X. Li, Z. Wu, V. D. Chakravarthy, and Z. Wu, A low-complexity approximation to lognormal sum distributions via transformed log skew normal distribution, IEEE Trans. Vehicular Technol. **60**, 4040 (2011).

[43] Z. Wu, X. Li, R. Husnay, V. Chakravarthy, B. Wang, and Z. Wu, A novel highly accurate log skew normal approximation method to lognormal sum distributions, in *2009 IEEE Wireless Communications and Networking Conference* (IEEE, New York, 2009), pp. 1–6.

[44] https://doi.org/10.5281/zenodo.4672142.

[45] N. H. Kuiper, Tests concerning random points on a circle, in Nederl. Akad. Wetensch. Proc. Ser. A **63**, 38 (1960).

[46] W. H. Press, S. A. Teukolsky, W. T. Vetterling, and B. P. Flannery, *Numerical Recipes in C* (Cambridge University Press, Cambridge, England, 1988).

[47] M. Gregg, H. Seim, and D. Percival, Statistics of shear and turbulent dissipation profiles in random internal wave fields, J. Phys. Oceanogr. **23**, 1777 (1993).

[48] M. A. Stephens, EDF statistics for goodness of fit and some comparisons, J. Am. Stat. Assoc. **69**, 730 (1974).